Impact of inner-wall reflection on UV reactor performance as evaluated by using computational fluid dynamics: The role of diffuse reflection

Wentao Li [a], Mengkai Li [a], James R. Bolton [b], Jiuhui Qu [a], Zhimin Qiang [a, *]

[a] Key Laboratory of Drinking Water Science and Technology, Research Center for Eco-Environmental Sciences, University of Chinese Academy of Sciences, Chinese Academy of Sciences, 18 Shuang-qing Road, Beijing, 100085, China
[b] Department of Civil and Environmental Engineering, University of Alberta, Edmonton, AB T6G 2W2, Canada

ABSTRACT

Making use of the reflected ultraviolet (UV) radiation with a reflective inner wall is a promising way to improve UV reactor performance. In this study, the impact of inner-wall reflection on UV reactor performance was evaluated in annular single-lamp UV reactors by using computational fluid dynamics, with an emphasis on the role of diffuse reflection. The UV radiation inside the reactor chamber was simulated using a calibrated discrete ordinates radiation model, which has been proven to be a reliable tool for modeling fluence rate (FR) distributions in UV reactors with a reflective inner wall. The results show that UV reactors with a highly reflective inner wall (*Reflectivity* = 0.80) had obviously higher FRs and reduction equivalent fluences (REFs) than those with an ordinary inner wall (*Reflectivity* = 0.26). The inner-wall diffuse reflection further increased the reactor REF, as a result of the elevated volume-averaged FR. The FR distribution uniformity had conditioned contributions to UV reactor performance. Specifically, in UV reactors with a plug-like flow the FR distribution uniformity contributed to the REF to some extent, while in UV reactors with a mixed flow it had little influence on the REF. This study has evaluated, for the first time, the impact of inner-wall diffuse reflection on UV reactor performance and has renewed the understanding about the contribution of FR distribution uniformity to UV reactor performance.

© 2016 Elsevier Ltd. All rights reserved.

1. Introduction

Ultraviolet (UV) technologies are being employed worldwide for water disinfection and purification because of their high efficiency in inactivating protozoa and generating oxidative hydroxyl radicals when used in combination with chemicals such as H_2O_2 (Hijnen et al., 2006; Esplugas et al., 2002; Xu et al., 2009). Microorganisms or pollutants are inactivated or degraded after receiving a sufficient UV fluence (or UV dose) when flowing through a UV reactor. To ensure an efficient fluence delivery, UV reactors are usually designed with the help of computational fluid dynamics (CFD). Configuration modifications, such as adding baffle plates, have been demonstrated to improve the performance of UV disinfection reactors by providing an optimized reactor hydrodynamics (Chiu et al., 1999), and a flow pattern closer to plug flow was found to lead to a higher pollutant degradation in UV reactors for advanced oxidation purpose (Sozzi and Taghipour, 2007). Wols et al. (2011) carried out a comprehensive investigation on the performances of UV reactors with various configurations (i.e., both microbial disinfection and pollutant degradation efficiencies) by taking account of the corresponding fluence distributions. They concluded that measures that increase the average fluence and/or narrow the fluence distribution, such as placing mirrors and adding static mixers, are beneficial to the UV reactor performance.

Among the measures to increase the average fluence of a UV reactor, making use of the reflected UV radiation with a reflector appears to be a promising strategy. Reflection can be of two types: *specular reflection*, where the UV light is reflected like that at a mirror; and *diffuse reflection*, where the UV light is reflected from a ragged surface in all directions. Sommer et al. (1996) found that the use of an aluminum reflector increased the reduction equivalent

* Corresponding author.
  E-mail address: qiangz@rcees.ac.cn (Z. Qiang).

Nomenclature

A	Surface area of quartz sleeve (m^2)
CFD	Computational fluid dynamics
CF_i	Individual calibration factor ($-$)
CF_u	Uniform calibration factor ($-$)
d_1	Reactor internal diameter (mm)
d_2	Reactor inlet (or outlet) internal diameter (mm)
DO	Discrete ordinates
e	Internal emissivity $-$ emission of thermal radiation ($-$)
E_o	Direct Irradiation on the radiation boundary (W m^{-2})
f_d	Diffuse fraction of inner-wall reflection ($-$)
F_0	Intercept of microbial fluence-response curve on X axis (mJ cm^{-2})
F_i	Fluence received by the ith particle (mJ cm^{-2})
F_{min}	Particle minimum fluence (mJ cm^{-2})
FDR	Fully diffuse reflection
FR	Fluence rate (mW cm^{-2})
FR_{aa}	Area-averaged fluence rate (mW cm^{-2})
FR_{max}	Maximum fluence rate (mW cm^{-2})
FR_{min}	Minimum fluence rate (mW cm^{-2})
FR_{va}	Volume-averaged fluence rate (mW cm^{-2})
FR_{wa}	Weighted average fluence rate (mW cm^{-2})
HRW	Highly reflective inner wall
k	Microbial UV inactivation rate constant (cm^2 mJ^{-1})
L_1	UV reactor length (mm)
L_2	Quartz sleeve length (mm)
L_3	Lamp arc length (mm)
MFSD	Micro-fluorescent silica detector
N	Total simulating particle number ($-$)
ORW	Ordinary inner wall
P	Lamp power (W)
PDR	Partially diffuse reflection
R	Reflectivity ($-$)
R_d	Diffuse reflectivity ($-$)
REF	Reduction equivalent fluence (mJ cm^{-2})
RSD	Relative standard deviation ($-$)
UVT	UV transmittance (%)
η	Lamp UVC efficiency (%)

fluence (REF) of a UV disinfection device by over 40% at a water UV transmittance (UVT) of 97%. Recently, with a rapid progress in UV light emitting diodes (UV-LEDs), UV reactors employing this new light source have been developed, and reflectors made of aluminum or other highly reflective materials have been applied to make the best use of UV radiation inside the reactor chamber (Hessling et al., 2016; Wurtele et al., 2011). Nevertheless, researches concerning how the reflected UV radiation contributes to the UV reactor performance are still very limited, compared to the abundant works discussing the effect of the reactor hydrodynamics (Sozzi and Taghipour, 2006a; Wols et al., 2011; Xu et al., 2013).

Two obstacles lie in the way of an in-depth understanding of the effect of the reflected UV radiation. On the one hand, many commonly used fluence rate (FR) distribution models, such as the multiple segment source summation model whose reliability has been widely accepted, do not include a component to calculate the reflected UV radiation; on the other hand, although some FR distribution models, such as the discrete ordinates (DO) radiation model, do account for the reflection from the reactor inner wall, their accuracies in FR distribution predictions have not been well evaluated (Liu et al., 2004). In fact, there have been contradictory results with regard to the accuracy of the DO radiation model. Liu et al. (2004) found that the DO radiation model significantly overestimated the FRs in the near-lamp region but underestimated the FRs in the near-wall region; however, Ho (2009) found that the predicted FR distributions by the DO radiation model agreed quite well with the experimental data.

Recently, Li et al. (2011) developed a micro-fluorescent silica detector (MFSD) with a small volume and 360° response, which is very suitable for in-situ measurements of FR distributions inside UV reactors. Consequently, the FR distributions predicted by numerical models can be readily verified with the MFSD measurements, even in UV reactors with a reflective inner wall (Li et al., 2012). Based on the in-situ measured FR data, they found that the weighted average FR (FR_{wa}) was almost doubled in a UV reactor when aluminum was used as the inner-wall material in place of stainless steel. Another important finding is that the diffuse reflection of the inner wall enhanced the FR distribution uniformity, and a more uniform FR distribution was believed to improve the UV reactor performance (Li et al., 2012). From this perspective, the inner wall of UV reactors

should be made of materials with a high diffuse reflectivity. Nevertheless, to date no further study has been conducted to elucidate the effects of inner-wall diffuse reflection on FR distributions and the resulting UV reactor performance.

In this study, the impact of inner-wall reflection on UV reactor performance was evaluated in annular single-lamp UV reactors by using CFD simulations, with an emphasis on the role of diffuse reflection. FR distributions inside the reactor chamber were predicted by a DO radiation model after being calibrated with in-situ measured FR data. The effects of inner-wall reflection on FR distributions and REF were examined with different inner walls, and the underlying reason for a better performance of UV reactors with a higher inner-wall diffuse reflection was explored. This study, for the first time, has evaluated the impact of inner-wall diffuse reflection on UV reactor performance and clarified the contribution of FR distribution uniformity.

2. Materials and methods

2.1. UV reactors

Two annular single-lamp UV reactors with different inlet and outlet positions were employed as the model UV reactors, which were denoted as the L-shape (Fig. 1a) and U-shape (Fig. 1b) UV reactors, respectively. The different reactor configurations lead to different hydrodynamics inside the reactors. The UV reactors had a length (L_1) of 400 mm and an internal diameter (d_1) of 95 mm. The length (L_2) of the quartz sleeve (23 mm o.d., >98% transmittance at 254 nm) was 347 mm while the lamp arc length (L_3) was 297 mm. The low-pressure mercury lamp (GL Type, XiashiWanhua Co., China) had an output power (P) of 16 W and UVC efficiency (η, at 254 nm) of 26%. The inlet and outlet had a same internal diameter (d_2) of 45 mm, and the distance from the outlet central axis to the reactor end was 50 mm. Two kinds of inner walls were simulated, that is, an ordinary inner wall (ORW) with a reflectivity (R) of 0.26 (typical of stainless steel) and a highly reflective inner wall (HRW) with $R = 0.80$ (typical of aluminum). The diffuse fraction (f_d) of the inner-wall reflection varied from 0.1 to 0.9, accounting for inner walls with various diffuse reflectivities.
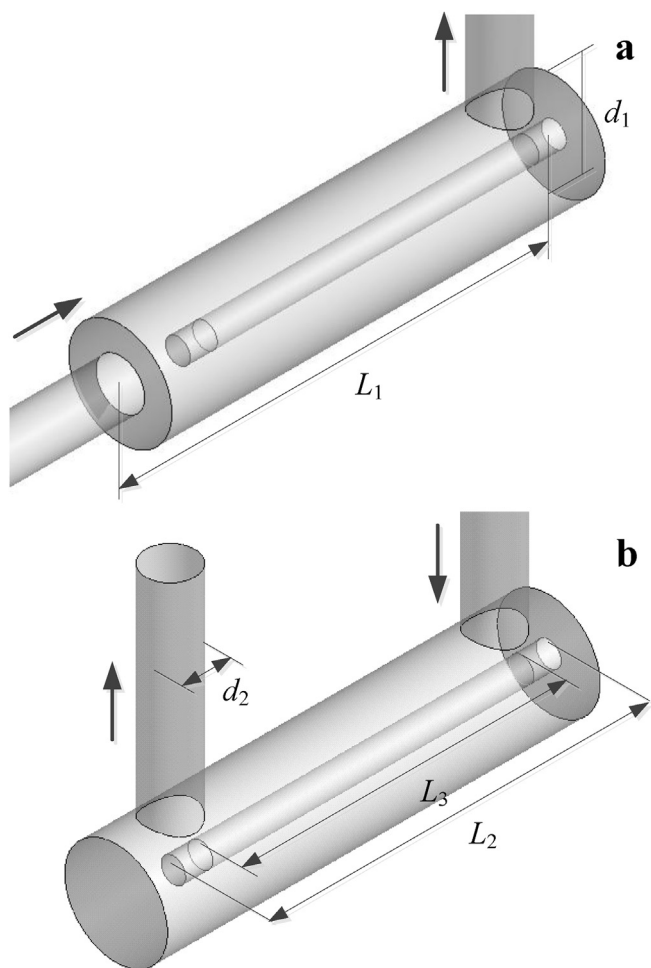
Fig. 1. Schematic diagram of the modeled UV reactors: (a) L-shape; and (b) U-shape.

2.2. Model settings

The hydrodynamics inside the UV reactors were modeled with the Realizable k-ε model, which has been proven to produce a reliable simulation of the flow field in annular UV reactors (Sozzi and Taghipour, 2006b). Unless otherwise specifically stated, the velocity at the reactor inlet was set at 0.1 m s^{-1}, which corresponded to a flow rate of 0.57 m^3 h^{-1}. The water UV transmittances were set at 99%, 90% and 75%, corresponding to the absorption coefficients of 1.0, 10.5 and 28.8 m^{-1}, respectively, in the model boundary conditions. The UV radiation was simulated by the DO radiation model, with the UV light assumed to be emitted from the quartz sleeve (Ho, 2009). According to the Fluent Manual (ANSYS, 2010), the reflectivity of an inner wall can be determined as follows:

$$R = 1 - e \tag{1}$$

$$R_d = f_d(1 - e) \tag{2}$$

where e = internal emissivity of the inner wall (i.e., emission of thermal radiation), R_d = diffuse reflectivity. Consequently, the various inner-wall reflections can be simulated by setting the e and f_d values accordingly. The e values were set at 0.74 and 0.20 for the ORW and HRW, respectively. Low, moderate and high inner-wall diffuse reflections were obtained by setting the f_d values at 0.1, 0.5 and 0.9, respectively. The microbial transportation and inactivation were simulated with the Lagrangian approach of the

Discrete Phase model by releasing more than 5000 simulating particles at the reactor inlet, and then their received fluences were calculated by a complied user-defined function (Ho et al., 2009). The REFs of the UV reactors were calculated following Eq. (3), assuming that the fluence-response of the challenge microorganism follows the delayed Chick-Watson model:

$$\text{REF} = -\frac{1}{k}\lg\left(\frac{1}{N}\sum_{i=1}^{N}10^{-k(F_i-F_0)}\right) + F_0 \tag{3}$$

where k = inactivation rate constant of the challenge microorganism (cm^2 mJ^{-1}), F_0 = intercept of the fluence-response curve on the X axis (mJ cm^{-2}), N = number of the total simulating micro particles, F_i = fluence received by the ith particle (mJ cm^{-2}). The challenge microorganism employed in this study was *Bacillus subtilis* spores (ATCC 6633). According to our previous study, the values of k and F_0 were determined to be 0.087 cm^2 mJ^{-1} and 3.0 mJ cm^{-2}, respectively (Qiang et al., 2013).

All the modeling processes were accomplished with the commercial CFD software package of ANSYS Fluent 13.0 (Canonsburg, PA, USA), and convergence of the solution was reached if the normalized residuals were all at a level of 10^{-5} or less. The model settings are detailed in Text S1 (see Supplementary Information).

2.3. Model calibration

Since there have been disputes about the accuracy of the DO radiation model in predicting FR distributions in UV reactors, a calibration was first conducted using the in-situ measured FR data. Instead of comparing the FRs of individual points inside the UV reactors as practiced by Qiang et al. (2013), FR$_{\text{wa}}$ was introduced in this study to calculate the calibration factor. This ensured an overall consistence of the results from the calibrated radiation model with the experimental data. The FRs of 11 test points with a radial distance to the sleeve ranging from 3 to 28 mm were employed to calculate the FR$_{\text{wa}}$ by considering their respective weighting factors (Text S2, see Supplementary Information) (Li et al., 2012). These test points were equidistantly distributed in the reactor chamber (Fig. S1) and thus could well represent the cross-sectional FR variations. The calibration factor for the DO radiation model was then determined as the ratio of the FR$_{\text{wa}}$ measured by the MFSD to that predicted by the model. Since the in-situ FR measurements were conducted in UV reactors with inner walls of a small diffuse reflectivity (Li et al., 2012), the f_d was set at 0.1 in the DO radiation model during the calibration process.

3. Results and discussion

3.1. Calibration of DO radiation model

The DO radiation model exhibited a general overestimation of the FRs in the UV reactors (Fig. S2), thus the calibration was very necessary. Table 1 presents the FR$_{\text{wa}}$ values determined by the MFSD (FR$_{\text{wa}}$-MFSD) and the DO radiation model (FR$_{\text{wa}}$-DO) for UV reactors with two inner-wall reflectivities (R = 0.26 and 0.80) at various water UVTs as well as the corresponding calibration factors. The individual calibration factors (CF$_i$) ranged from 0.77 to 0.84 at high UVTs (i.e., 90% and 99%) and 0.91 to 0.92 at UVT of 75%. Because the effect of inner-wall reflection was notable only at high UVTs, a uniform calibration factor (CF$_u$) of 0.80 was adopted, mainly accounting for the CF$_i$ values at UVTs of 90% and above (typical for drinking water). The CF$_u$ was then introduced into the Direct Irradiation calculations in the boundary condition settings (Eq. (4)), which caused a 20% reduction in the overall FR as calculated by the

Table 1
Weighted average fluence rates (FR$_{wa}$, mW cm^{-2}) for UV reactors with two inner-wall reflectivities ($R = 0.26$ and 0.80) at various water UVTs and the corresponding calibration factors for the DO radiation model. The diffuse fraction (f_d) was set at 0.1 in the DO radiation model.

Parameter	R = 0.26			R = 0.80		
	99%	90%	75%	99%	90%	75%
FR$_{wa}$-MFSD	10.76	7.35	4.65	23.18	10.20	5.42
FR$_{wa}$-DO	13.35	8.78	5.06	30.25	13.20	5.93
CF$_i$	0.81	0.84	0.92	0.77	0.77	0.91
CF$_u$			0.80			

FR$_{wa}$-MFSD: FR$_{wa}$ determined by the MFSD; FR$_{wa}$-DO: FR$_{wa}$ determined by the DO radiation model; CF$_i$: individual calibration factor; and CF$_u$: uniform calibration factor.

calibrated DO radiation model.

$$E_o = \mathrm{CF}_u \frac{P\eta}{A} \tag{4}$$

where E_o = Direct Irradiation on the radiation boundary (W m^{-2}), P = lamp power (W), η = lamp UVC efficiency, A = surface area of the quartz sleeve (m^2).

The radial FR distributions in the central planes of UV reactors with two inner-wall reflectivities at various water UVTs are shown in Fig. 2. The predicted FR distributions by the calibrated DO radiation model agreed well with the measured data by the MFSD, regardless of the inner-wall reflectivities. At UVTs of 90% and 99%, the relative deviations between the predicted and measured FR$_{wa}$ were all less than 5% (Fig. 2a and b), while at UVT = 75%, the relative

deviations became a little larger (about 13%) (Fig. 2c), which is reasonable since the CF$_u$ was determined based on the CF$_i$ values at high UVTs. Good agreements between the predicted and the measured data were also found for the axial FR distributions, in both the near-lamp and the near-wall regions (data not shown). This demonstrates that the calibrated DO radiation model can be a reliable tool for UV radiation simulations in UV reactors with a reflective inner wall. The accurate prediction of FR distributions by the calibrated DO radiation model facilitated the following analysis of the effects of inner-wall reflection on FR distributions and REF.

3.2. Effect of inner-wall reflection on FR distributions

Fig. 3 shows the radial FR distributions in the central planes of UV reactors with two inner-wall reflectivities and three f_d values (0.1, 0.5, and 0.9) at various water UVTs. Compared to those with the ORW (i.e., $R = 0.26$), the FRs in UV reactors with the HRW (i.e., $R = 0.80$) increased significantly at high UVTs and even almost doubled at UVT = 99% (Fig. 3a and b). This is because at a higher UVT, more UV radiation reaches the inner wall and then is reflected back into the reactor chamber by the HRW. The effect of inner-wall diffuse reflection on FR distributions was negligible in UV reactors with the ORW (Fig. 3c and e); however, with the HRW at high UVTs,
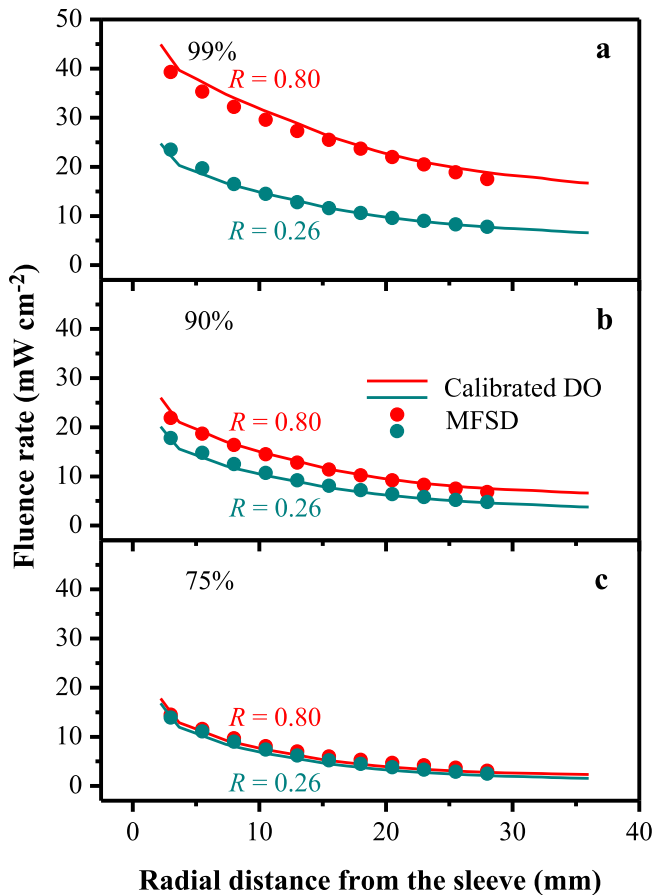

Fig. 2. Radial fluence rate (FR) distributions in the central planes of UV reactors with two inner-wall reflectivities ($R = 0.26$ and 0.80) at various water UVTs as determined by both the calibrated DO radiation model and the MFSD: (a) 99%; (b) 90%; and (c) 75%. The diffuse fraction (f_d) was set at 0.1 in the calibrated DO radiation model.
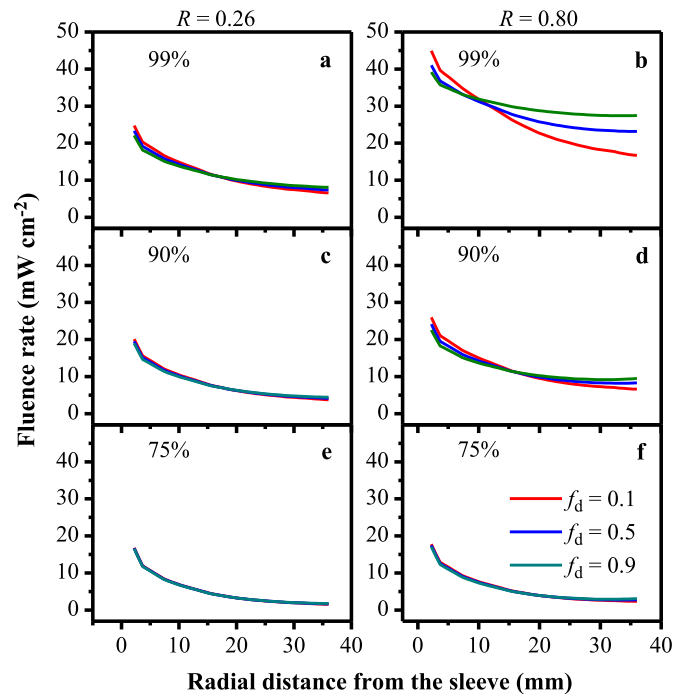

Fig. 3. Radial FR distributions in the central planes of UV reactors with two inner-wall reflectivities ($R = 0.26$ and 0.80) and three f_d values (0.1, 0.5 and 0.9) at various water UVTs: (a, b) 99%; (c, d) 90%; and (e, f) 75%.

the FR distributions became obviously more uniform as the f_d increased (Fig. 3b and d). This can be ascribed to the fact that the diffusely reflected UV light returned to the reactor chamber in all directions. Consequently, the optical path lengths were extended in the near-wall region but reduced in the near-lamp region, resulting in increased FRs near the wall and decreased FRs close to the lamp. These findings are in accordance with those reported by Li et al. (2012), and an improvement made here is that the effect of the diffuse reflection was demonstrated directly and quantitatively.

Table 2 shows the characteristic parameters of FR distributions in the central planes of UV reactors with two inner-wall reflectivities and three f_d values at various water UVTs. It was found that at UVT = 99%, both the area-averaged FR (FR_{aa}) in the central planes and the volume-averaged FR (FR_{va}) were more than doubled when the inner-wall reflectivity increased from 0.26 to 0.80. For UV reactors with a higher inner-wall diffuse reflection (i.e., a greater f_d), the relative standard deviation (RSD) of the cross-sectional FR decreased by having an increased minimum FR (FR_{min}) and a decreased maximum FR (FR_{max}). In the UV reactor with the HRW and $f_d = 0.9$ at UVT = 99%, the FR_{min} even increased to be about 60% of the FR_{max}, leading to the lowest RSD of 0.138. Therefore, diffuse reflection at high UVTs can greatly enhance the FR distribution uniformity in UV reactors with a highly reflective inner wall. A uniform FR distribution has been traditionally treated as a promoter for the UV reactor performance. It should be noted that the FR_{va} also increased with increasing f_d, with the largest increase being 19%. This is because with a higher inner-wall diffuse reflection, more UV radiation was retained in the reactor chamber by having an increased axial optical path length. The elevated FR_{va} can further improve the UV reactor performance.

3.3. Effect of inner-wall reflection on REF

The REFs of UV reactors with various inner-wall reflections are shown in Fig. 4. In either type of UV reactor (i.e., the L-shape or the U-shape), considerable REF increments were found with the HRW as compared to those with the ORW. For example, at UVT = 90%, a typical UVT for drinking water treatment, the REF was raised by 42–64% for the L-shape UV reactors and by 44–55% for the U-shape UV reactors; and at UVT = 99%, the REF was even raised by
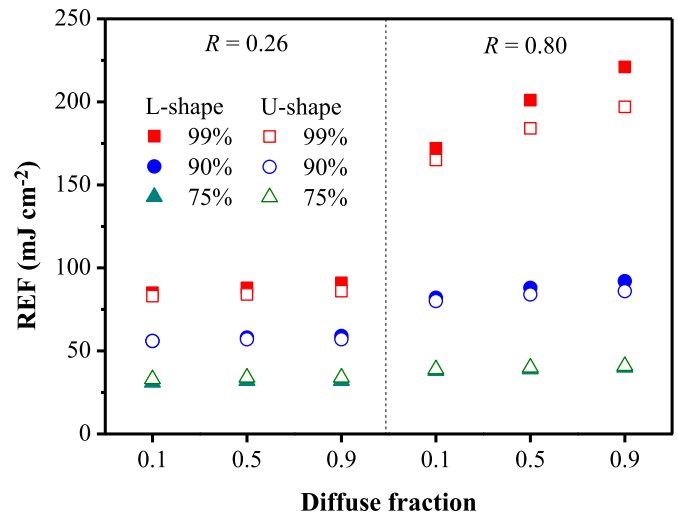

Fig. 4. REFs of UV reactors with two inner-wall reflectivities ($R = 0.26$ and 0.80) and three f_d values (0.1, 0.5 and 0.9) at various water UVTs. The solid and open symbols indicate the results of the L-shape and U-shape UV reactors, respectively.

103–161% and 99–138%, respectively. This can be attributed to the significantly elevated FR_{va} values in UV reactors with the HRW. In fact, the REF increments in both types of UV reactors with the HRW were comparable to the FR_{va} increments, which were 49–57% at UVT = 90% and 130–175% at UVT = 99% (Table 2). Chen et al. (2011) found a 24% increment in the microbial log inactivation at UVT = 92% when the inner-wall reflectivity increased from 0 to 0.6 in a cross-flow UV reactor. This increment is relatively lower as compared to the results in this study, mainly arising from a much larger inlet water velocity (i.e., 0.86 m s^{-1}) adopted in their study, which resulted in a flush flow in the reactor chamber that could not make full use of the reflected UV radiation.

As the f_d increased, the REF increments in UV reactors with the ORW were negligible (i.e., <7%), while those in UV reactors with the HRW were as large as 19–28%. The effect of f_d on the reactor performance can also be seen from the corresponding fluence distributions (Fig. S3). For UV reactors with the HRW, the fluence distributions obviously shifted to higher fluences as the f_d increased (Figs. S3a and b); by contrast, the fluence distributions of UV reactors with the ORW had little shift regardless of the f_d (Figs. S3c and d). As mentioned above, both the enhanced FR distribution uniformity and the elevated FR_{va} could contribute to the REF increment. To clarify their individual role, the ratios of the FR_{va} and REF with $f_d = 0.5$ and 0.9 to those with $f_d = 0.1$ in UV reactors with the HRW at various water UVTs were analyzed (Fig. 5). It was found that at all the three UVTs, the percent increases of the REF in the L-shape UV reactors were a little higher than those of the FR_{va}; however, in the U-shape UV reactors they were almost the same. Taking the case of UVT = 99% for example, the FR_{va} was increased by 21% in UV reactors with $f_d = 0.9$, while the percent REF increases were 28% and 19%, respectively, in the L-shape and U-shape UV reactors. Therefore, the inner-wall diffuse reflection had varied effects on the UV reactor performance, which depended on the reactor configuration. For the U-shape UV reactors, the performance improvement was in line with the FR_{va} increment resulting from the inner-wall diffuse reflection; while for the L-shape UV reactors, the enhanced FR distribution uniformity could have a further contribution to the UV reactor performance. This can be ascribed to the different hydrodynamics in the two types of UV reactors. As illustrated in Fig. S4, the flow pattern in the L-shape UV reactor was close to a plug flow. In this situation, the particle

Table 2
Characteristic parameters for FR distributions in the central planes and FR_{va} values (mW cm^{-2}) of UV reactors with two inner-wall reflectivities and three f_d values (0.1, 0.5 and 0.9) at various water UVTs.

Parameter	$R = 0.26$			$R = 0.80$		
	$f_d = 0.1$	$f_d = 0.5$	$f_d = 0.9$	$f_d = 0.1$	$f_d = 0.5$	$f_d = 0.9$
UVT = 99%						
FR_{aa}	10.61	10.74	10.88	23.73	26.37	29.36
FR_{max}	32.55	30.91	29.44	52.88	47.82	45.44
FR_{min}	6.11	6.88	7.57	15.95	22.18	26.75
RSD	0.566	0.496	0.434	0.390	0.220	0.138
FR_{va}	7.60	7.65	7.72	17.51	19.31	20.87
UVT = 90%						
FR_{aa}	7.08	7.11	7.14	10.58	10.92	11.24
FR_{max}	28.41	27.73	27.08	34.60	32.40	30.55
FR_{min}	3.44	3.79	4.11	6.13	7.76	8.89
RSD	0.774	0.732	0.692	0.612	0.500	0.413
FR_{va}	5.05	5.06	5.08	7.51	7.72	7.91
UVT = 75%						
FR_{aa}	4.25	4.25	4.26	4.96	4.99	5.02
FR_{max}	25.98	25.84	25.73	27.06	26.62	26.21
FR_{min}	1.39	1.51	1.61	2.11	2.49	2.76
RSD	1.227	1.212	1.198	1.070	1.026	0.986
FR_{va}	3.05	3.05	3.05	3.55	3.57	3.59

FR_{aa}: area-averaged FR (mW cm^{-2}); FR_{max}: maximum FR (mW cm^{-2}); FR_{min}: minimum FR (mW cm^{-2}); and RSD: relative standard deviation.
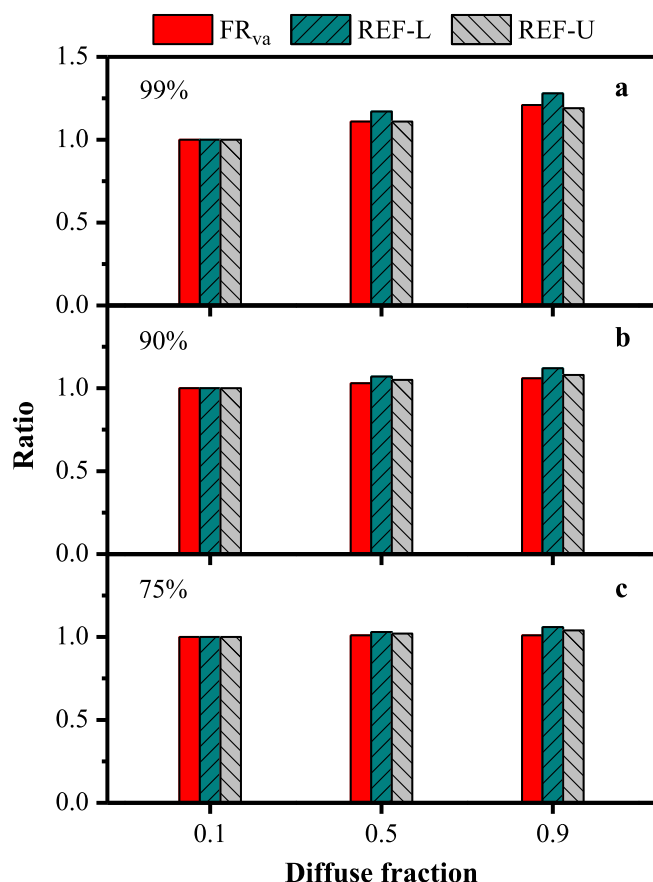
Fig. 5. Ratios of the volume-averaged FR (FR_{va}) and REF with $f_d = 0.5$ and 0.9 to those with $f_d = 0.1$ in UV reactors with a highly reflective inner wall at various water UVTs: (a) 99%; (b) 90%; and (c) 75%. The REF-L and REF-U represent the REFs of the L-shape and U-shape UV reactors, respectively.

minimum fluence (F_{min}), which plays a determinant role in the REF (Li et al., 2016), would most probably be found with particles traveling in the near-wall region. Because the FR_{va} increment was a net result of the FR increase in the near-wall region subtracting the FR decrease in the near-lamp region, the degree of increase in the F_{min} was slightly greater than that in the FR_{va}. Consequently, the percent increase of the REF was a little higher than that of the FR_{va}. In contrast, the F_{min} in the U-shape UV reactor would most probably be found with particles in the flush flow that crossed over both the near-lamp and the near-wall regions. Consequently, the F_{min} would have a similar degree of increase to the FR_{va}, which resulted in similar percent increases of the REF and the FR_{va}.

3.4. Contribution of FR distribution uniformity to UV reactor performance

The result that the FR distribution uniformity had a limited contribution to the UV reactor performance is somewhat unexpected, since creating a uniform UV radiation has traditionally been viewed as an effective measure to improve the UV reactor performance (Schoenen, 1996). To confirm the above finding, a UV reactor with an utmost uniform FR distribution was created by making the inner wall 100% reflective (i.e., $R = 1$) with a fully diffuse reflection (i.e., $f_d = 1$) (denoted as the FDR UV reactor), and its performance was compared to that of a common UV reactor with a partially diffuse reflection (i.e., $R = 0.26$, $f_d = 0.1$) (denoted as the PDR UV reactor). The FR_{va} in the two UV reactors was kept identical at

6.30 mW cm^{-2} to rule out its interference. The radial FR distributions in the two UV reactors at UVT = 99% are shown in Fig. S5. Results indicate that the FRs in the central plane of the PDR UV reactor decreased dramatically from 32.55 to 6.11 mW cm^{-2} (RSD = 0.576), while those of the FDR UV reactor only varied from 13.38 to 10.74 mW cm^{-2} (RSD = 0.050).

The REFs of the PDR and FDR UV reactors at UVT = 99% with different flow rates are shown in Fig. 6. With the L-shape configuration, the FDR UV reactor had a 12% higher REF than the PDR UV reactor; while with the U-shape configuration, the two UV reactors had identical REFs (Fig. 6a). As the flow rate increased from 0.57 to 1.15 m^3 h^{-1}, the REF of the FDR UV reactor was increased by 19% as compared to that of the PDR UV reactor with the L-shape configuration; however, the REFs of the two UV reactors with the U-shape configuration were still the same (Fig. 6b). This is due to the fact that as the flow rate increased, the flow pattern became more like a plug flow in the L-shape UV reactor, while it remained as a mixed flow in the U-shape UV reactor. Therefore, the FR distribution uniformity made a conditioned contribution to the UV reactor performance. To be specific, in UV reactors with a plug-like flow (e.g., the L-shape UV reactor), the FR distribution uniformity contributed notably to the REF (12—19%); while in UV reactors with a mixed flow (e.g., the U-shape UV reactor), the FR distribution uniformity had little influence on the REF. The different performances of the PDR and FDR UV reactors with L-shape and U-shape configurations were also manifested by their corresponding fluence distributions (Fig. S6). In accordance with the slightly higher REFs, the F_{min} values in the FDR UV reactors with the L-shape configuration were a little larger than those in the PDR UV reactors (Figs. S6a and c). On the other hand, no significant difference was found in the fluence distributions between the FDR and PDR UV
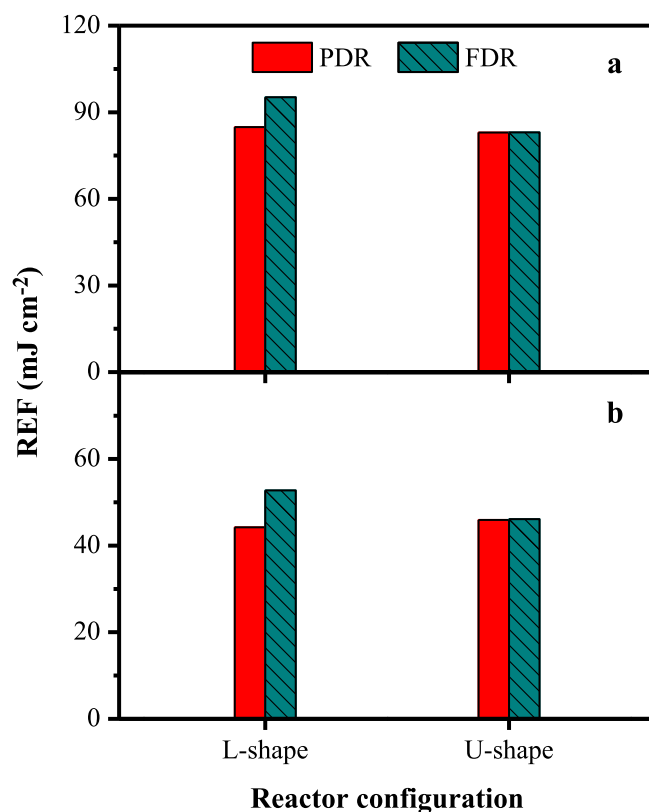

Fig. 6. REFs of PDR and FDR UV reactors with two configurations at water UVT = 99% at different flow rates: (a) 0.57 m^3 h^{-1}; and (b) 1.15 m^3 h^{-1}.

reactors with the U-shape configuration (Figs. S6b and d), which agreed well with the REF results in Fig. 6.

3.5. Implications

The inner-wall reflection in UV reactors can significantly increase the FR_{va} and the corresponding REF, and the higher the inner-wall reflectivity is, the greater improvement of the UV reactor performance can be achieved. Therefore, employing a highly reflective inner wall can be an efficient approach to improve the UV reactor performance, which will eventually increase the UV reactor treatment capacity and reduce the specific cost. The reflective inner wall can be directly made of a highly reflective material, or be realized following the structure of UV reactors with UV-LEDs (i.e., a reflector is put behind a quartz tube).

The inner-wall diffuse reflection makes a further contribution to the UV reactor performance. Nevertheless, this benefit is only notable (19–28%) with a highly reflective inner wall ($R = 0.80$) at UVT = 99%, and a higher f_d usually means an increased roughness, which causes the inner wall more likely to be fouled. As a result, it is not advisable to improve the UV reactor performance by increasing the inner-wall diffuse reflectivity. For the first time, the FR distribution uniformity has been proven to make a conditioned contribution to the UV reactor performance, and in common UV reactors with a mixed flow, the FR distribution uniformity has little impact on the UV reactor performance. Therefore, concerning the UV reactor design, more attention should be paid to the hydrodynamics and the FR_{va} rather than the FR distribution uniformity.

4. Conclusions

The impact of inner-wall reflection on the UV reactor performance was evaluated in annular single-lamp UV reactors by using CFD simulations, with a special focus on the role of diffuse reflection. The FR distributions inside the UV reactors were simulated with a calibrated DO radiation model. The effects of inner-wall reflection on the FR distributions and REF were investigated, and the contribution of FR distribution uniformity to the UV reactor performance was clarified. The main conclusions included:

- The FR distributions in UV reactors with a reflective inner wall could be predicted accurately with the calibrated DO radiation model, with the relative deviations between the predicted and measured FR_{wa} values being less than 5% at high water UVTs ($\geq$90%).
- The FRs in UV reactors with the HRW (i.e., $R = 0.80$) were significantly higher than those with the ORW (i.e., $R = 0.26$), especially at high water UVTs. The inner-wall diffuse reflection enhanced the FR distribution uniformity and increased the FR_{va} at the same time.
- The REF increment of UV reactors with the HRW was considerable and highly related with the FR_{va} increment. The inner-wall diffuse reflection further increased the reactor REF, which mainly arose from the elevated FR_{va}.
- The FR distribution uniformity had conditioned contributions to the UV reactor performance. In the L-shape UV reactors with a plug-like flow, the FR distribution uniformity contributed notably to the REF increment (12–19%); however, in the U-shape UV reactors with a mixed flow, the FR distribution uniformity had little influence on the REF.

Appendix A. Supplementary data

Supplementary data related to this article can be found at http://dx.doi.org/10.1016/j.watres.2016.11.068.

References

ANSYS, 2010. ANSYS FLUENT 13.0 Theory Guide. ANSYS Inc., Canonsburg, PA, USA.

Chen, J., Deng, B.Q., Kim, C.N., 2011. Computational fluid dynamics (CFD) modeling of UV disinfection in a closed-conduit reactor. Chem. Eng. Sci. 66 (21), 4983–4990.

Chiu, K., Lyn, D.A., Savoye, P., Blatchley III, E.R., 1999. Effect of UV system modifications on disinfection performance. J. Environ. Eng. 125 (5), 459–469.

Esplugas, S., Gimenez, J., Contreras, S., Pascual, E., Rodriguez, M., 2002. Comparison of different advanced oxidation processes for phenol degradation. Water Res. 36 (4), 1034–1042.

Hessling, M., Gross, A., Hoenes, K., Rath, M., Stangl, F., Tritschler, H., Sift, M., 2016. Efficient disinfection of tap and surface water with single high power 285 nm LED and square quartz tube. Photonics 3 (1), 7.

Hijnen, W.A.M., Beerendonk, E.F., Medema, G.J., 2006. Inactivation credit of UV radiation for viruses, bacteria and protozoan (oo) cysts in water: a review. Water Res. 40 (1), 3–22.

Ho, C.K., 2009. Evaluation of reflection and refraction in simulations of ultraviolet disinfection using the discrete ordinates radiation model. J. Water Sci. Technol. 15 (12), 2421–2428.

Ho, C.K., Khalsa, S.S., Wright, H.B., Wicklein, E., 2009. Modeling UV disinfection using integrated computational fluid dynamics and discrete ordinates radiation models. Proc. Water Environ. Fed. 2009 (1), 257–273.

Li, M.K., Qiang, Z.M., Li, T.G., Bolton, J.R., Liu, C.L., 2011. In situ measurement of UV fluence rate distribution by use of a micro fluorescent silica detector. Environ. Sci. Technol. 45 (7), 3034–3039.

Li, M.K., Qiang, Z.M., Bolton, J.R., Ben, W.W., 2012. Impact of reflection on the fluence rate distribution in a UV reactor with various inner walls as measured using a micro-fluorescent silica detector. Water Res. 46 (11), 3595–3602.

Li, W.T., Li, M.K., Bolton, J.R., Qiang, Z.M., 2016. Configuration optimization of UV reactors for water disinfection with computational fluid dynamics: feasibility of using particle minimum UV dose as a performance indicator. Chem. Eng. J. 306, 1–8.

Liu, D., Ducoste, J.J., Jin, S., Linden, K., 2004. Evaluation of alternative fluence rate distribution models. Aqua J. Water Supply Res. Technol. 53 (6), 391–408.

Qiang, Z.M., Li, M.K., Bolton, J.R., Qu, J.H., Wang, C., 2013. Estimating the fluence delivery in UV disinfection reactors using a 'detector-model' combination method. Chem. Eng. J. 233, 39–46.

Schoenen, D., 1996. The influence of inhomogenous irradiation in UV disinfection-experimental findings and theoretical considerations. J. Water Supply Res. Technol. AQUA 45 (3), 120–129.

Sommer, R., Cabaj, A., Haider, T., 1996. Microbicidal effect of reflected UV radiation in devices for water disinfection. Water Sci. Technol. 34 (7–8), 173–177.

Sozzi, D.A., Taghipour, F., 2006a. UV reactor performance modeling by Eulerian and Lagrangian methods. Environ. Sci. Technol. 40 (5), 1609–1615.

Sozzi, D.A., Taghipour, F., 2006b. Computational and experimental study of annular photo-reactor hydrodynamics. Int. J. Heat. Fluid Fl 27 (6), 1043–1053.

Sozzi, A., Taghipour, F., 2007. The importance of hydrodynamics in UV advanced oxidation reactors. Water Sci. Technol. 55 (12), 53–58.

Wols, B.A., Hofman, J.A.M.H., Beerendonk, E.F., Uijttewaal, W.S.J., van Dijk, J.C., 2011. A systematic approach for the design of UV reactors using computational fluid dynamics. AIChE J. 57 (1), 193–207.

Wurtele, M.A., Kolbe, T., Lipsz, M., Kulberg, A., Weyers, M., Kneissl, M., Jekel, M., 2011. Application of GaN-based ultraviolet-C light emitting diodes-UV LEDs-for water disinfection. Water Res. 45 (3), 1481–1489.

Xu, B., Gao, N.Y., Cheng, H.F., Xia, S.J., Rui, M., Zhao, D.D., 2009. Oxidative degradation of dimethyl phthalate (DMP) by UV/H2O2 process. J. Hazard. Mater. 162 (2–3), 954–959.

Xu, C., Zhao, X.S., Rangaiah, G.P., 2013. Performance analysis of ultraviolet water disinfection reactors using computational fluid dynamics simulation. Chem. Eng. J. 221, 398–406.